Supportive Information

1. Chemicals

Sodium formate (≥ 99 %), NADH disodium salt (≥ 84 %), NAD^+ (≥ 95 %), di-potassium hydrogen phosphate (≥ 99 %) and potassium dihydrogen phosphate (≥ 99 %) were purchased from Carl Roth (Karlsruhe, Germany). The enzyme formate dehydrogenase (FDH) from *Candida boidinii* (75 U/mL in 3.2 M ammonium sulphate) was purchased from Megazyme (Bray, Ireland). Pierce 660 nm protein assay reagent was purchased at Thermo Scientific (Waltham, USA). The epoxy functionalized resin for enzyme immobilization (Lifetech ECR 8204M epoxy resin) was purchased from Purolite (King of Prussia, USA).

2. Immobilization Procedure

To recycle and stabilize the enzyme for a variety of experiments, it was immobilised on a methyl acrylate epoxy resin. For the immobilization of FDH on Lifetech ECR 8204M epoxy resin, 1 mL of the enzyme suspension was centrifuged for 10 min with 21382 g at 4°C. The supernatant was saved for enzyme concentration measurements and the pellet was resuspended with 500 mM potassium phosphate buffer (KP_i), pH 8, to a total volume of 10 mL with an enzyme concentration of 1.9 mg/mL. 328.8 mg of epoxy resins were washed four times with 1 mL of 500 mM KP_i, pH 8, for resin equilibration. The equilibrated enzyme carrier was placed into the enzyme solution. The mixture was gently stirred in a rotary shaker for 23 hours at 4°C to prevent enzyme deactivation. Subsequently, the immobilised enzyme was vacuum filtrated and washed with 50 mM KP_i, pH 8. The washing procedure was carried out in eight steps with 1 mL buffer each. To determine the immobilization yield, the enzyme concentration of the initial enzyme solution and all wash solutions was measured resulting in an immobilisation yield of 49.7 %. The activity yield of the immobilisates resulted in an active enzyme loading of 3.7 U per gram carrier. These were filled into the packed bed reactor of the automated reactor system.

3. UV/Vis Calibration

For the determination of NADH concentration, the maximum absorbance of nine samples (ranging between 0 and 2 mM NADH) were measured at 340 nm within a 1 mm flow-through cuvette. The samples were pumped through the cuvette for a minute at a rate of 1 mL per minute. To compensate for wavelength spreads during flow measurement, the maximum absorption with a 10 nm wavelength spread was applied for concentration calculation. The spectrometer intensity was measured using the Seabreeze Python package (Poehlmann, 2019). The integration time was 0.1 s, and five measurement points were averaged for the steady-state concentration of NADH. To ensure accurate readings, the cuvette was flushed with 50 mM pH 8 phosphate buffer between measurements. Calibration data, including the slope, intercept, and baseline, were stored in a JSON file (Equation 1). The absorbance was calculated using the baseline intensity (equation 2), which involved the subtraction of the baseline to correct it (cf. Figure 1).

3.1 Calibration Calculations

$$A = ac + b \quad (1)$$

Absorbance

$$A = \log_{10} \frac{I_0}{I_i} \quad (2)$$

Limit of Detection (LoD)

$$LoD(c) = \frac{3.3\sigma}{a} \quad (3)$$

Limit of Quantification (LoQ)

$$LoQ(c) = \frac{10\sigma}{a} \quad (4)$$

A= Absorbance

a = slope

c = concentration of NADH

b = Intercept

σ = standard deviation

I_0 = Baseline intensity

I_i = Measured intensity

3.2 NADH Spectrum

The absorbance of NADH is measured at 340 nm with a spread of ± 10 nm to account for variations due to the flow setup. A typical spectrum showing the region of interest is shown in Figure 1.

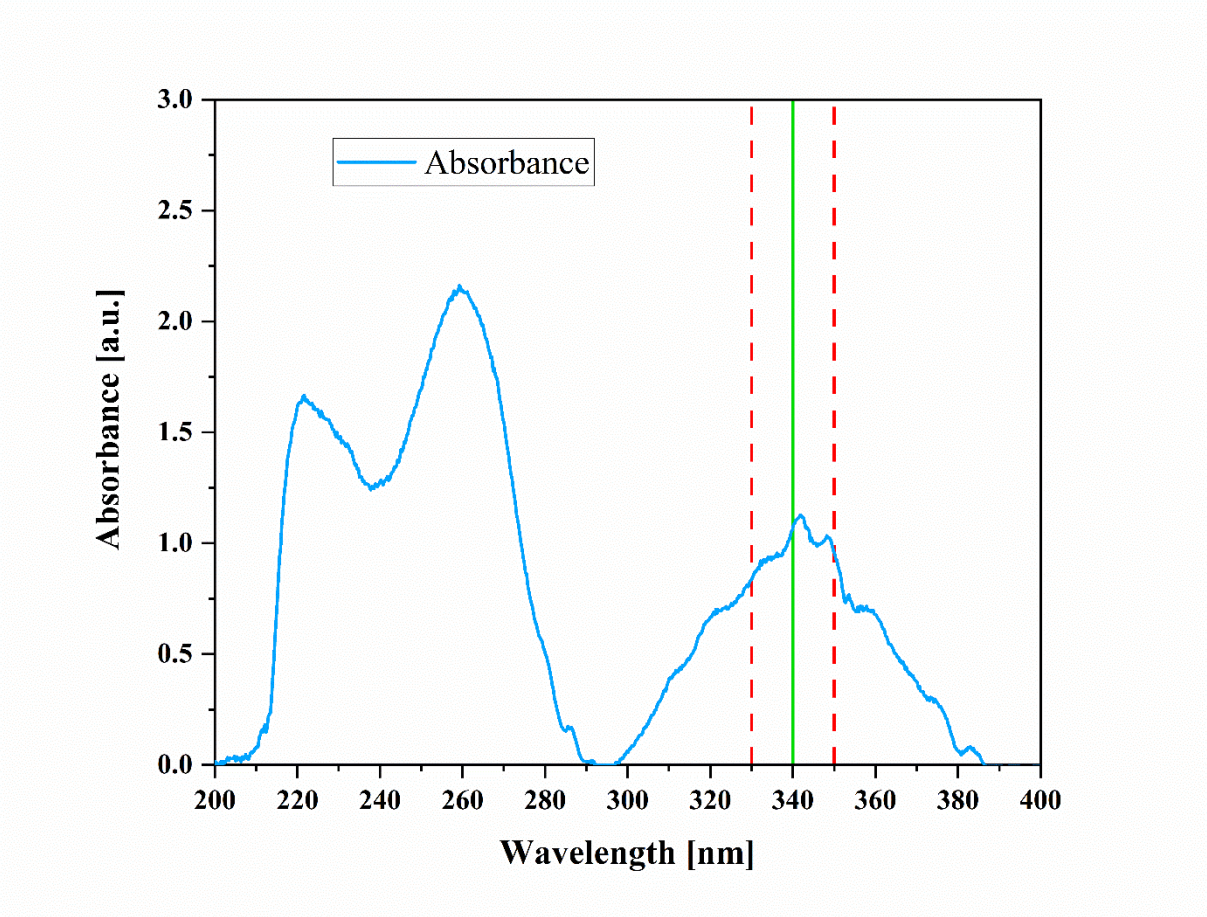

Figure 1 UV/Vis spectrum during a reaction of 1 mM NAD^+ and 150 mM sodium formate with a NADH concentration of 0.89 mM in a 1 mm flow-through cuvette.

3.3 Closed-loop Calibration

For the closed-loop setup, the spectrometer was calibrated with NADH solutions ranging from 0 to 2 mM.

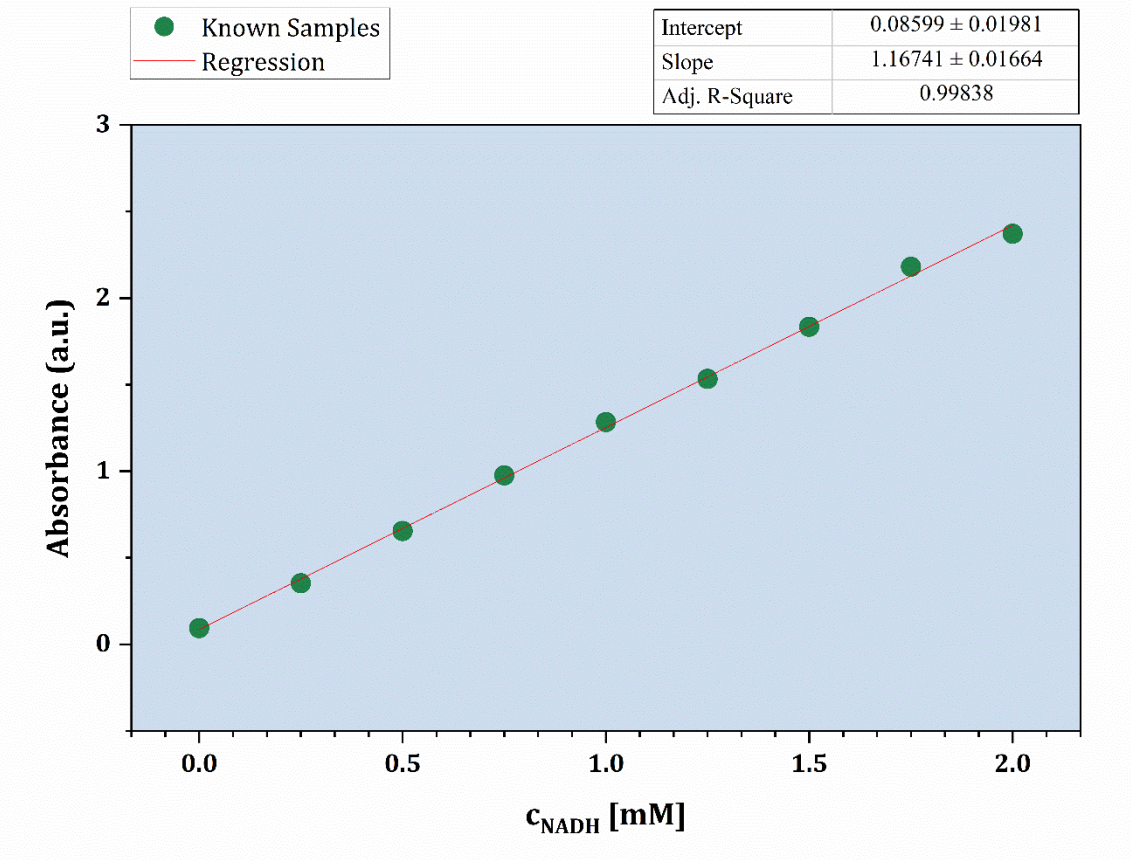

Figure 2 Calibration curve for NADH at 340 nm for the closed-loop determination of the product concentration in a 1 mm flow through cuvette. The concentration range is 0 mM to 2 mM NADH in 50 mM KP_i buffer pH 8. The absorbance for the calibration curves are raw values.

The LoD of 0.047 mM and a LoQ of 0.143 mM results when applying the calibration curve method with a slope of 1.167 mM^{-1} and a standard deviation of 0.017 mM^{-1} (cf. equation 3 and 4).

3.4 Calibration for Extended Range

To extend the design space of the closed-loop setup, an offline UV/Vis spectrophotometer (Shimadzu UV-1280, Duisburg, Germany) was calibrated with NADH solutions ranging from 0 to 10 mM.

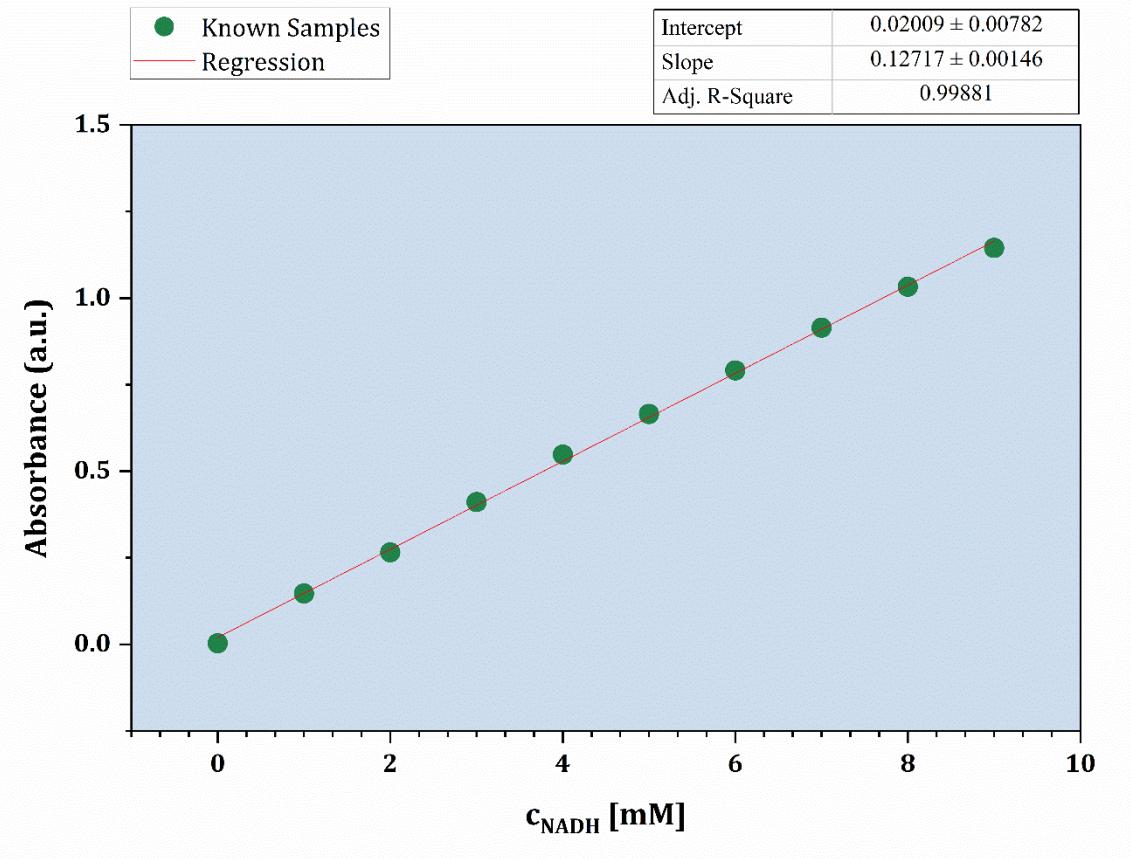

Figure 3 Calibration curve for NADH at 380 nm for the determination of the product concentration of the extended design space up to 10 mM NAD^+. The concentration range is 0 mM to 9 mM NADH in 50 mM KP_i buffer. LoD = 0.038 mM and LoQ = 0.115 mM

3.5 NAD^+ Calibration and Deactivation

For the measurement of NAD^+ concentration, a temperature controlled UV/Vis spectrometer was calibrated at 300 nm in the range of 0 to 4 mM NAD at 24 °C. For the measurement, a 10 mm quartz cuvette was used.

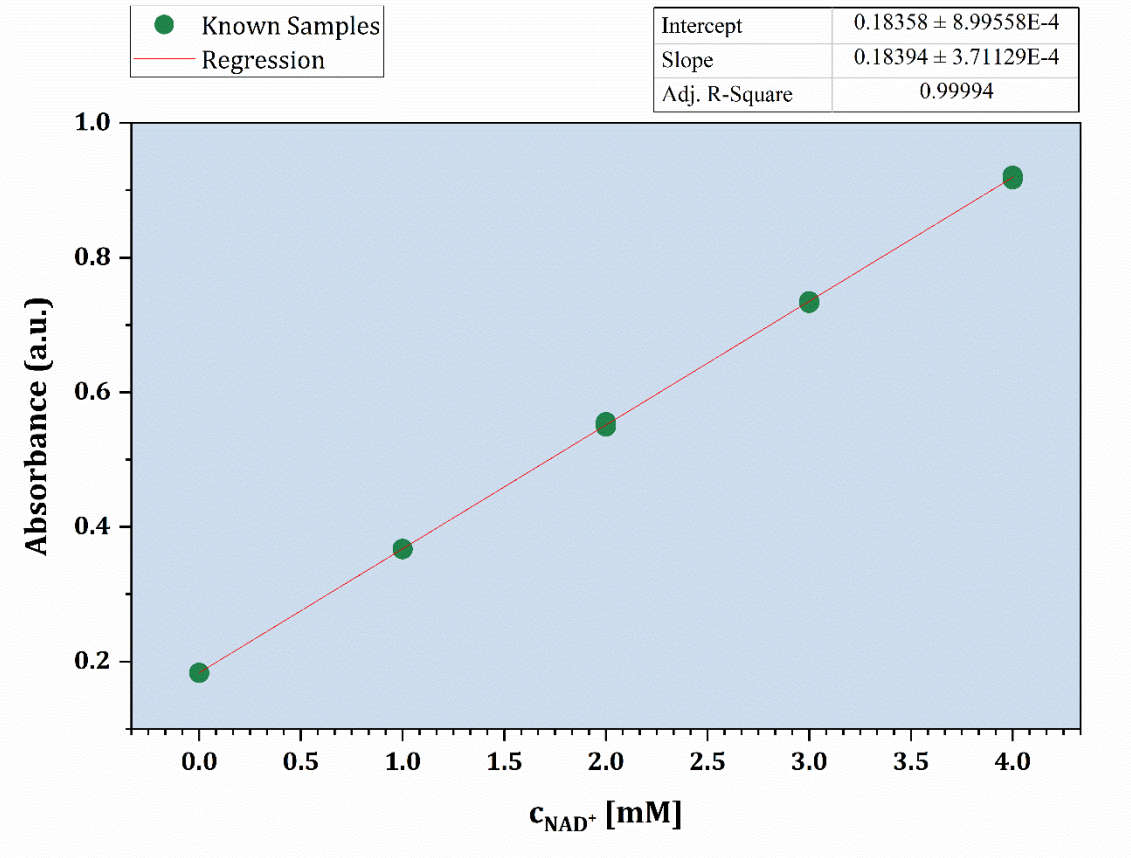

Figure 4 Calibration curve for NAD^+ at 300 nm for the determination of the NAD^+ concentration for the evaluation of the thermal decay of NAD^+. The concentration range is 0 mM to 4 mM NADH in 50 mM KP_i buffer. All measurements were performed in triplicates. LoD = 0.007 mM and LoQ = 0.02 mM.

To determine the NAD^+ deactivation rate, 4.1 mM NAD^+ in 50 mM KP_i at pH 8 was monitored for a period of six hours, which is the standard campaign length of the closed-loop reactor platform. The rate of change was analysed with the conventional exponential decay (first order) and with a linear decay (zero order) models to ascertain the deactivation rate. In this timeframe, the model fits yielded in $R^2_{adjusted}$ = 0.9398 and $R^2_{adjusted}$ = 0.9394 for the first and zero-order, respectively (cf. Figure 5). Due to the small difference, the zero order model was selected to explain the deactivation with a deactivation constant of 0.000275 $mM \cdot min^{-1}$.

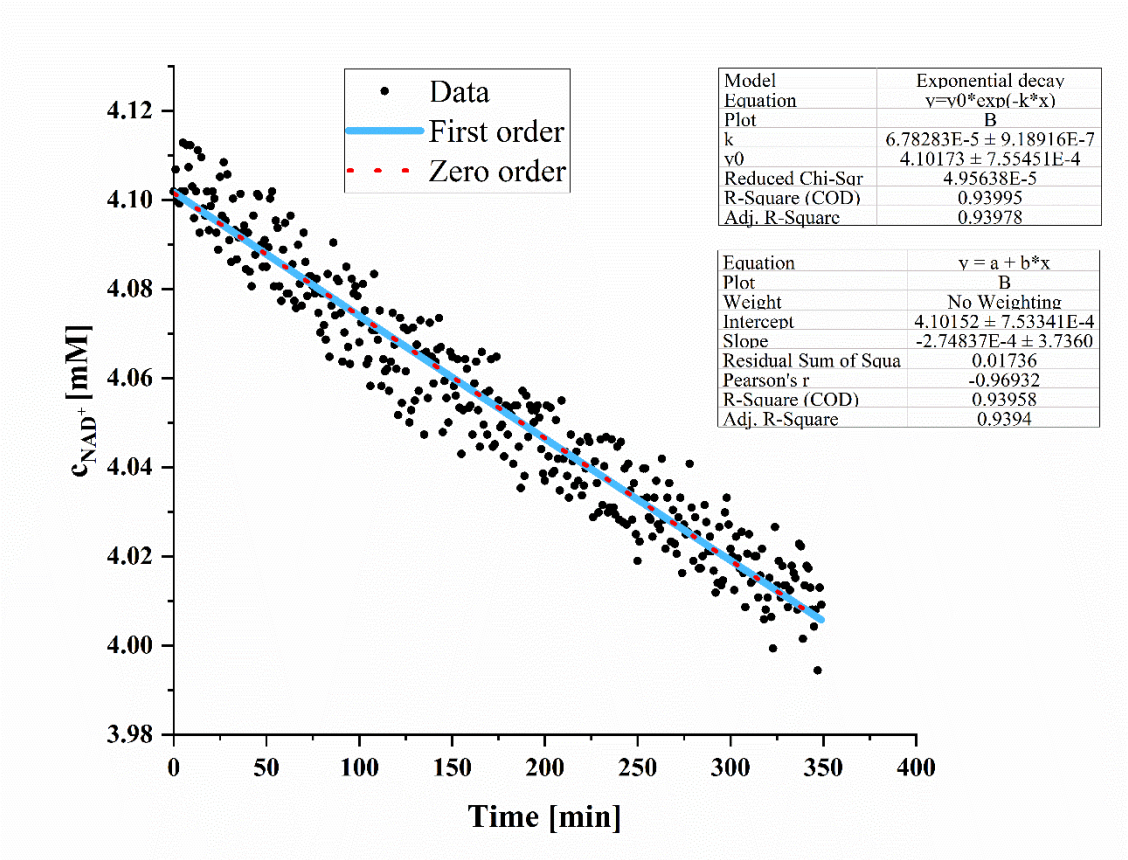

Figure 5 Fitting of first and zero order kinetics to the decaying concentration of NAD+ in 50 mM KP_i at pH 8 and 24 °C for 6 hours. The measurement was performed at 300 nm applying a 1 cm quartz cuvette in temperature controlled spectrometer (UvikonXL, Bio-Tek Instruments, Bad Friedrichshall, Germany).

4. Workflow of Model-Based Design of Experiments

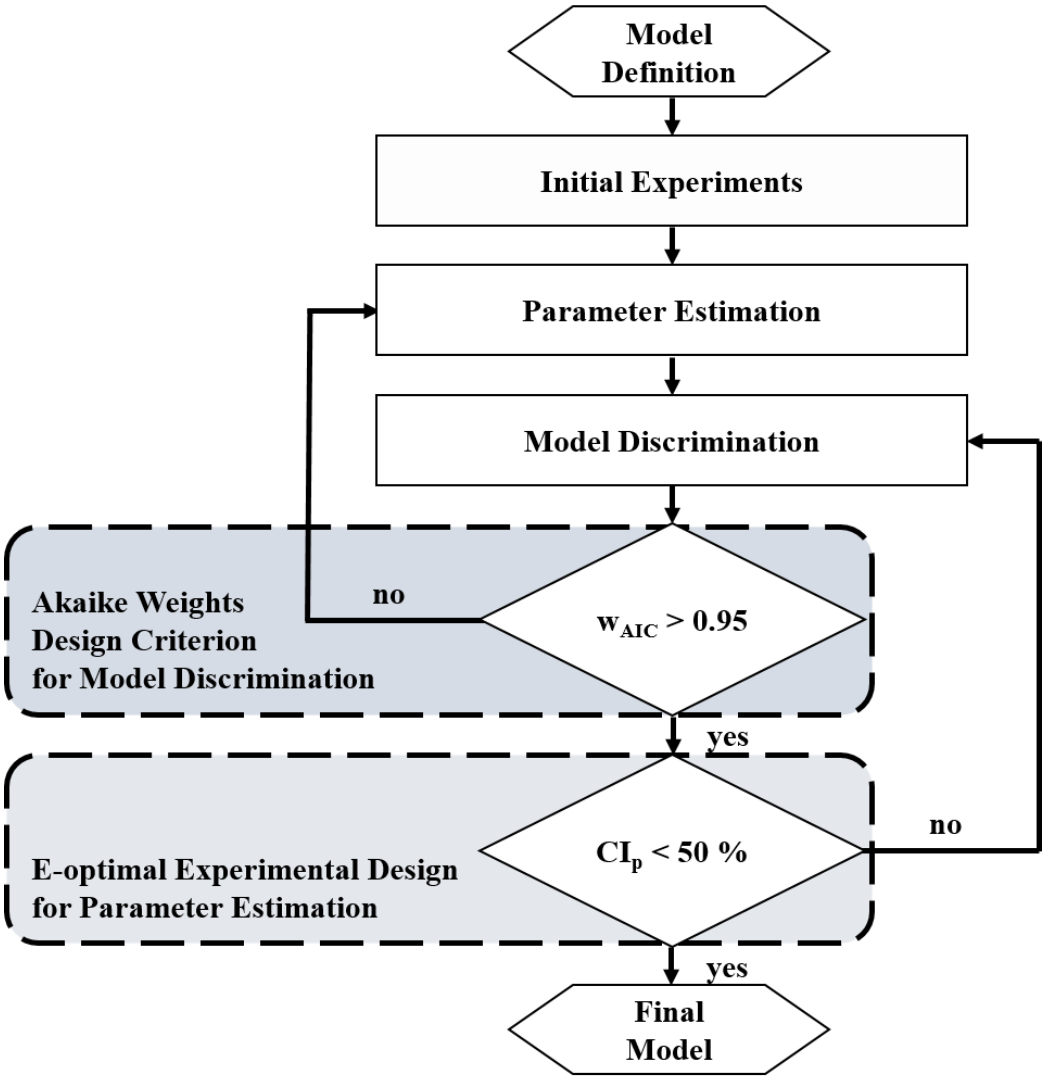

Figure 6 Systematic Workflow for the Model-Based Design of Experiments based on the AWDC criterion.

The workflow was performed using self-written Python and MATLAB scripts, which are available at the Open-Access Repository of the Hamburg University of Technology (TORE) with the URL: https://doi.org/10.15480/882.9427.

Within DesignOfExperiments.m, detailed information about the calculation procedure is given as comments in the script.

4.1 Breakdown of the Workflow

1.) Model Definition
   - Reactor modelled as plug flow reactor implemented by means of an ordinary differential equation system and solved as initial value problem by means of the *ode45* solver in Matlab
   - Proposition of candidate models following different rate laws
   - Specification of initial parameter estimates
2.) Initial Experiments
   - Several initial experiments are performed by varying inlet concentrations
   - Outlet concentration for individual experiments are determined with UV/Vis-spectrometer
3.) Parameter Estimation
   - Table of input data (inlet concentrations) and response data (output concentrations) is prepared for nonlinear parameter regression
   - Application of nonlinear least-square curve-fitting (*lsqcurvefit*) in Matlab for parameter regression
   - Parameter regression performed for each individual model candidates
   - Calculation of 95%-confidence intervals with *coefCI*
4.) Model Discrimination
   - Estimation of Akaike information criterion (AIC) for all models
   - AIC based on loglikelihood values with penalty term for complexity of model (number of model parameter)
   - Selection of best model with Akaike weights ($0 < w_{AIC} < 1$)
5.) Optimal Experimental Design
   - Determine the next best experiments for model identification
   - The non-linear optimization problem is solved with *fmincon*
   - Selection between two objective criteria:
     a) Optimal Experimental Design for Model Discrimination ($w_{AIC} < 0.95$)
        - If no model reaches Akaike weight of $w_{AIC} > 0.95$, model discrimination is not satisfied and no clear distinction between models possible
        - Goal is design new experiments which help to improve discrimination power
        - Previous parameter estimates used to forecast model responses
        - Objective criterion: Maximize deviation between model responses
     b) Optimal Experimental Design for Parameter Estimation ($w_{AIC} > 0.95$ & $CI_p < 50\%$)
        - If one model reaches $w_{AIC} > 0.95$, model discrimination is considered successful
        - Then parameter estimates of selected model are checked
        - If confidence intervals of selected model are higher than 50% ($CI_p < 50\%$), the precision of the parameter estimates is considered insufficient
        - Goal is to design new experiments to maximise the precision of the parameter estimates
        - Fisher Information Matrix is used to approximate the variance of the parameter estimates
        - Objective criterion: E-Optimally = Maximize minimal Eigenvalue of Fisher Information Matrix
6.) Final Model

When all stop criteria for model discrimination and parameter estimation are fulfilled, the final model is built.

4.2 Model Simulation

The model simulation was performed with an increased design space for the NAD^+ concentration of 0 to 40 mM to visualize the approximation of the maximum reaction rate in the PBR:

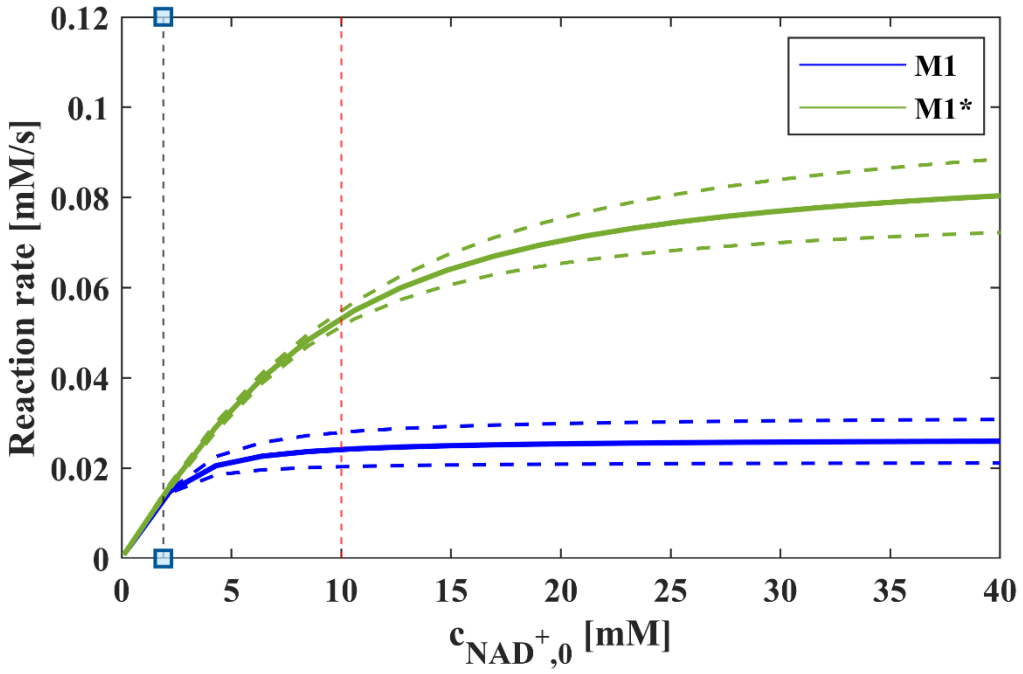

Figure 7 Simulation of reaction rates over the initial NAD^+ concentration for a constant formate concentration of 300 mM. M1 represents the model after closed-loop experiments and M1* represents the corrected model after the extension of the design space. The prediction was prolonged to 40 mM NAD^+. The original design space is indicated with a black dashed line and the extended design space is indicated with a red dashed line.

At a concentration of 40 mM NAD^+, the rise in the reaction rate of M1* is significantly low, indicating that the maximum reaction rate has been approximated. This concentration is unsuitable for industrial usage, which also applies to the reactor system. This remains valid even at 10 mM NAD^+, while this concentration was needed to compensate for the high level of active enzyme in the PBR. Although shorter residence times could have been used to solve this problem, it was not possible in the current configuration. Another option would have been to use a shorter PBR, which would decrease the enzyme usage and backpressure of the PBR, but this was not available.

5. Control Software

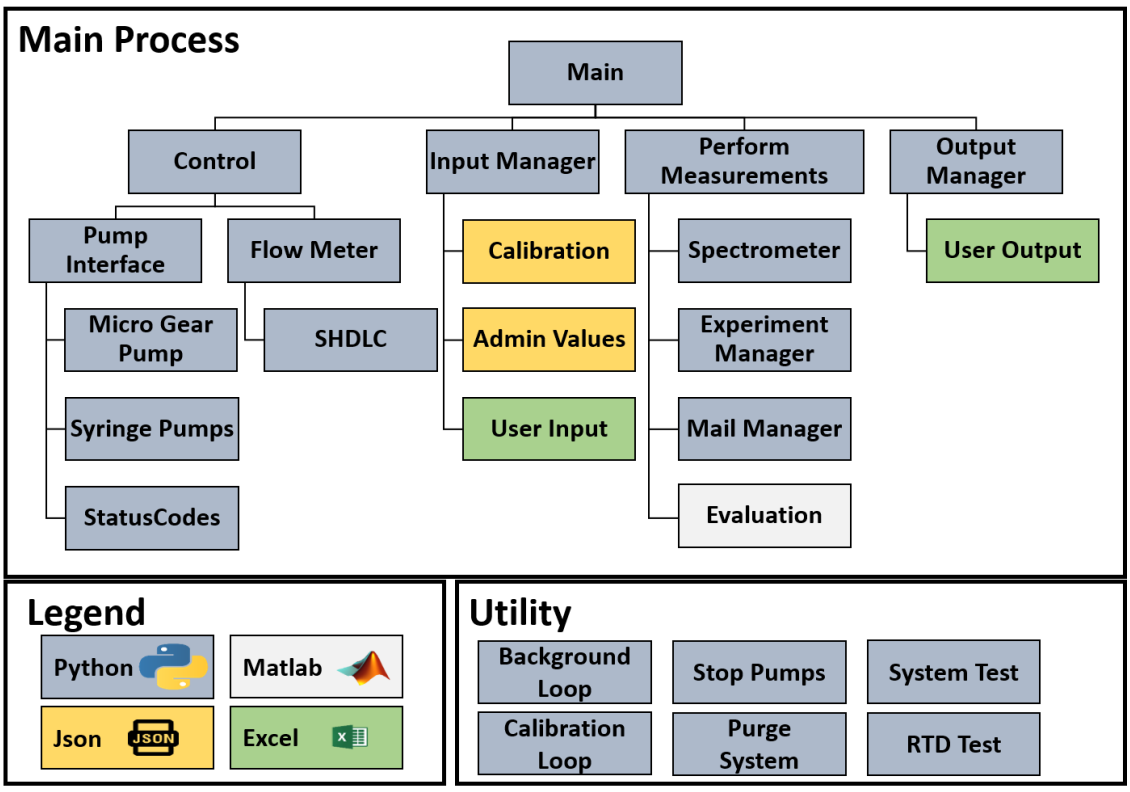

Figure 8 Simplified control software hierarchy written in Python with Json and Excel files as Input. The MATLAB script is implemented for the model identification and model-based design of experiment by Lucas Schaare.

With the initialization of the main script, the experimental platform was started. The defined initial DoE with six experiments were given the "User Input" excel file and conducted with the settings defined in "Admin values". The measurements of the NADH concentration were conducted after the defined amount of residence times. After that, the model discrimination was conducted with the MATLAB script. Based on the results, new experiments were designed and added to the experimental list, to increase the model discrimination. When the threshold for the model discrimination (weighted AIC ≥ 0.95) was reached, the objective function was changed to improve the parameter estimation with the e-optimal design criterion. One run was finished when either the maximum amount of experiments were performed (15) or the threshold for the parameter estimation was reached (95 %-confidence intervals of <50 %).

5. Closed-loop Data

Table 1 NADH steady state concentrations of different experimental campaigns in the PBR setup. MBDoE 1 and MBDoE 2 refer to the campaigns described in the publication. AWDC and CDC indicate the experiments of the extended design space.

Experiment	No.	c_{NAD}	$c_{formate}$	τ	c_{NADH}
MBDoE-1.1	1	1.000	150.0	2	0.935
MBDoE-1.1	2	0.350	50.0	2	0.266
MBDoE-1.1	3	0.350	290.0	2	0.327
MBDoE-1.1	4	1.900	50.0	2	1.372
MBDoE-1.1	5	1.900	290.0	2	1.602
MBDoE-1.1	6	1.000	150.0	2	0.917
MBDoE-1.1	7	1.883	50.0	2	1.413
MBDoE-1.1	8	1.805	275.5	2	1.543
MBDoE-1.1	9	1.137	50.0	2	0.966
MBDoE-1.1	10	1.805	275.5	2	1.536
MBDoE-1.1	11	1.871	50.0	2	1.403
MBDoE-1.1	12	1.805	275.5	2	1.545
MBDoE-1.1	13	1.116	50.0	2	0.962
MBDoE-1.1	14	1.805	275.5	2	1.544
MBDoE-1.1	15	1.860	50.0	2	1.377
MBDoE-1.2	16	1.000	150.0	2	0.901
MBDoE-1.2	17	0.350	50.0	2	0.292
MBDoE-1.2	18	0.350	290.0	2	0.315
MBDoE-1.2	19	1.900	50.0	2	1.231
MBDoE-1.2	20	1.900	290.0	2	1.580
MBDoE-1.2	21	1.000	150.0	2	0.889
MBDoE-1.2	22	1.883	50.0	2	1.383
MBDoE-1.2	23	1.805	275.5	2	1.519
MBDoE-1.2	24	1.112	50.0	2	0.981
MBDoE-1.2	25	1.805	275.5	2	1.534
MBDoE-1.2	26	1.871	50.0	2	1.373
MBDoE-1.2	27	1.805	275.5	2	1.524
MBDoE-1.2	28	1.865	50.0	2	1.381
MBDoE-1.2	29	1.805	275.5	2	1.511
MBDoE-1.2	30	1.860	50.0	2	1.388
MBDoE-1.3	31	1.000	150.0	2	0.886
MBDoE-1.3	32	0.350	50.0	2	0.292
MBDoE-1.3	33	0.350	290.0	2	0.318
MBDoE-1.3	34	1.900	50.0	2	1.298
MBDoE-1.3	35	1.900	290.0	2	1.541
MBDoE-1.3	36	1.000	150.0	2	0.904
MBDoE-1.3	37	1.883	50.0	2	1.353
MBDoE-1.3	38	1.805	275.5	2	1.495
MBDoE-1.3	39	1.128	50.0	2	0.965

MBDoE-1.3	40	1.805	275.5	2	1.487
MBDoE-1.3	41	1.871	50.0	2	1.352
MBDoE-1.3	42	1.805	275.5	2	1.509
MBDoE-1.3	43	1.865	50.0	2	1.337
MBDoE-1.3	44	1.805	275.5	2	1.499
MBDoE-1.3	45	1.860	50.0	2	1.339
Full Factorial	46	0.350	50.0	2	0.265
Full Factorial	47	0.350	133.3	2	0.278
Full Factorial	48	0.350	216.7	2	0.273
Full Factorial	49	0.350	300.0	2	0.302
Full Factorial	50	0.900	50.0	2	0.743
Full Factorial	51	0.900	133.3	2	0.788
Full Factorial	52	0.900	216.7	2	0.808
Full Factorial	53	0.900	300.0	2	0.824
Full Factorial	54	1.450	50.0	2	1.135
Full Factorial	55	1.450	133.3	2	1.219
Full Factorial	56	1.450	216.7	2	1.249
Full Factorial	57	1.450	300.0	2	1.270
Full Factorial	58	1.900	50.0	2	1.357
Full Factorial	59	1.900	133.3	2	1.501
Full Factorial	60	1.900	216.7	2	1.561
Full Factorial	61	1.900	300.0	2	1.574
MBDoE-2.1	62	1.000	150.0	2	0.900
MBDoE-2.1	63	0.350	50.0	2	0.318
MBDoE-2.1	64	0.350	290.0	2	0.316
MBDoE-2.1	65	1.900	50.0	2	1.364
MBDoE-2.1	66	1.900	290.0	2	1.595
MBDoE-2.1	67	1.000	150.0	2	0.906
MBDoE-2.1	68	0.445	64.5	2	0.388
MBDoE-2.1	69	0.445	64.5	2	0.400
MBDoE-2.1	70	0.445	64.5	2	0.391
MBDoE-2.1	71	0.445	64.5	2	0.399
MBDoE-2.1	72	0.445	64.5	2	0.396
MBDoE-2.1	73	0.445	64.5	2	0.396
MBDoE-2.1	74	0.445	64.5	2	0.387

MBDoE-2.1	75	0.445	64.5	2	0.411
MBDoE-2.1	76	0.445	64.5	2	0.407
MBDoE-2.2	77	1.000	150.0	2	1.011
MBDoE-2.2	78	0.350	50.0	2	0.347
MBDoE-2.2	79	0.350	290.0	2	0.369
MBDoE-2.2	80	1.900	50.0	2	1.451
MBDoE-2.2	81	1.900	290.0	2	1.705
MBDoE-2.2	82	1.000	150.0	2	1.007
MBDoE-2.2	83	0.445	64.5	2	0.441
MBDoE-2.2	84	0.445	64.5	2	0.456
MBDoE-2.2	85	0.445	64.5	2	0.433
MBDoE-2.2	86	0.445	64.5	2	0.452
MBDoE-2.2	87	0.445	64.5	2	0.436
MBDoE-2.2	88	0.445	64.5	2	0.451
MBDoE-2.2	89	0.445	64.5	2	0.437
MBDoE-2.2	90	0.445	64.5	2	0.439
MBDoE-2.2	91	0.445	64.5	2	0.453
Error	92	1.000	150.0	2	0.932
Error	93	0.350	50.0	2	0.332
Error	94	0.350	290.0	2	0.331
Error	95	1.900	50.0	2	1.381
Error	96	1.900	290.0	2	1.595
Error	97	1.000	150.0	2	0.931
SCHM	98	1.000	150.0	2	0.893
SCHM	99	0.350	50.0	2	0.315
SCHM	100	0.350	290.0	2	0.301
SCHM	101	1.900	50.0	2	1.331
SCHM	102	1.900	290.0	2	1.603
SCHM	103	1.000	150.0	2	0.918
SCHM	104	1.883	50.0	2	1.345
SCHM	105	1.805	275.5	2	1.534
SCHM	106	1.119	50.0	2	0.995
SCHM	107	1.805	275.5	2	1.530
SCHM	108	1.871	50.0	2	1.332
SCHM	109	1.805	275.5	2	1.532
SCHM	110	1.865	50.0	2	1.341
SCHM	111	1.805	275.5	2	1.522
SCHM	112	1.860	50.0	2	1.329
AWDC/CDC	113	10.000	10.0	2	1.806
AWDC	114	3.500	1.0	2	0.497
Extra	115	0.400	7.0	2	0.275
AWDC/CDC	116	10.000	1500.0	2	6.788

6. References

Poehlmann, A. (**2019**) *Python Seabreeze*. Available at: https://python-seabreeze.readthedocs.io/en/latest/.